Heliyon 8 (2022) e12533

Contents lists available at ScienceDirect

Heliyon

journal homepage: www.cell.com/heliyon

Research article

Inflammatory and pathological changes in *Escherichia coli* infected mice

Nana Long [a,b,1], Jingzhu Deng [a,b,1], Min Qiu [a,b,1], Yanjiao Zhang [a,b], Yuzhen Wang [a,b], Wei Guo [a,b], Min Dai [a,b,*], Lin Lin [a,b,**]

[a] School of Laboratory Medicine, Chengdu Medical College, Chengdu, Sichuan, PR China
[b] Sichuan Provincial Engineering Laboratory for Prevention and Control Technology of Veterinary Drug Residue in Animal-origin Food, Chengdu Medical College, Chengdu, 610500, Sichuan, PR China

ARTICLE INFO

Keywords:
Escherichia coli
Infection
Inflammatory response
Pathological tissue

ABSTRACT

Purpose: Understanding the inflammation and histopathological changes in vivo caused by *Escherichia coli* infection is of great significance for scientific research and clinical diagnosis.

Methods: Mice were randomly divided into 6 groups (N = 10) after adaptive feeding, and it challenged by intraperitoneal injection with different concentrations of *E. coli* ATCC25922. The survival situation within 7 days was recorded, and the half-lethal dose (LD_{50}) was calculated by Karber's method. After the end, the blood, heart, liver, spleen, lung, and kidney of the mice were collected. We detected the concentration of inflammatory cytokines (IL-6, IL-β, and TNF-α) and inducible nitric oxide synthase (iNOS) in serum by ELSIA. Organs were observed by histopathological staining and electron microscope observation.

Results: The LD_{50} of mice infected with *E. coli* was $1.371*10^6$ CFU/kg. The concentrations of IL-6, IL-β, and TNF-α increased with time after infection in mice, reaching the highest concentration on the 7th day. iNOS was significantly increased on the 1st day of infection, and then decreased over time ($P < 0.01$). Within a week after infection, the colony counts of the heart, liver, spleen, lung and kidney showed a first decrease, and then reached a surge on the 7th day. Pathological results showed that a small amount of mitochondrial swelling and autophagy were seen in the spleen, lung and kidney tissues of the infected group; and a small amount of secondary lysosomes and autophagy were also seen; but no pathological changes were found in the liver and heart.

Conclusion: *Escherichia coli* can cause inflammation and oxidative stress in mice, causing different degrees of damage to the spleen, lung, and kidney tissues, which provides theoretical support for inflammatory and pathological changes caused by *Escherichia coli* infection in vivo.

1. Introduction

Escherichia coli (E. coli) colonizes the intestines of humans and other warm-blooded animals. *E. coli*, which was one of the most important pathogens for hospital infections, animal infections, food poisoning and water pollution [1, 2], it spreads widely among people, animals, and the environment [3, 4]. Clinically, *E. coli* can cause a variety of clinical diseases in all age groups [5], including diarrhea, urinary tract infections, bacteremia, meningitis, septicemia and pneumonia [6].

In order to fight pathogens, the immune system is activated, leading to the release of pro-inflammatory cytokines and the recruitment of inflammatory cells [7]. IL-6, IL-β and TNF-α play important roles in coordinating innate immune response [8]. TNF-α, is a cytokine produced mainly by activated macrophages, and a kind of pro-inflammatory cytokines that can up-regulate the expression of IL-6 and IL-1βand increase the permeability of epithelial cells [9], jointly complete the task of removing invaders. On the other hand, upon the triggering of immunologic or inflammatory stimulus, iNOS can produce most of the NO in vivo to defend invading infectious pathogens, meanwhile, iNOS is contribute to antigen-specific T cells and NK cells secrete TNF-α, IL-1β and IL-6 to defend pathogen infection [10].

Therefore, the establishment of a model of mouse infection with *E. coli* is convenient for understanding the dynamic changes during the infection process for in-depth research in the future.

* Corresponding author.
** Corresponding author.
E-mail addresses: daimin1015@cmc.edu.cn (M. Dai), linlin@cmc.edu.cn (L. Lin).
[1] Contributed equally.

https://doi.org/10.1016/j.heliyon.2022.e12533
Received 30 August 2022; Received in revised form 31 October 2022; Accepted 14 December 2022

2. Material and methods

2.1. Establish a mouse model of E. coli infection

We purchased KM mice (SPF grade) mice, weighing 18–22 g, half male and half female. After one week of feeding, they were randomly divided into 6 groups according to their body weight, with 10 rats in each group, and divided into 5 experimental groups and 1 blank group. The standard strain of *E. coli* ATCC25922 (presented by Sichuan Antibiotics Industry Research Institute) was activated, propagated, and then inoculated in solid nutrient agar for cultivation. The standard strain of *E. coli* ATCC25922 was cultured at a constant temperature at 37 °C to the logarithmic phase. The bacterial solution was diluted with physiological saline into five bacterial solutions with different concentration gradients, and the blank group was injected with physiological saline solution (The dosage is shown in Figure 1), and KM mice were injected intraperitoneally. The mortality of mice in the experimental group within 72 h was recorded. Statistic results of death rate, calculated half lethal dose (LD_{50}). Preparation of infection model mice: KM mice (SPF) were injected intraperitoneally with LD_{50} bacterial solution to prepare a mouse model of *E. coli* infection. All animal experiments were conducted in accordance with the principles of good laboratory animal care and performed in compliance with the Animal Ethics Review Committee of Chengdu Medical College.

2.2. Changes in inflammatory response and oxidative stress levels in mouse models of E. coli infection

We collected blood from mice injected with LD_{50} bacterial solution to detect inflammatory factors. The inflammatory factor interleukin-1β (IL-1β), Interleukin-6 (IL-6), tumor necrosis factor (TNF-α) and inducible nitric oxide synthase (iNOS) levels were determined according to the instructions of the ELISA kit (NEOBIOSCIENCE, ShenZhen, CHINA).

2.3. Fluctuation of Escherichia coli in organs of mice after infection

The mice were sacrificed after ether anesthesia, and the heart, liver, spleen, kidney, lung and other tissues were weighed and homogenized. The homogenates were serially diluted in phosphate-buffered saline and inoculatedoned MacConkey agar plates, whichwere incubated at 37 °C over night and then the numbers of bacterial colonies were counted.

2.4. Pathological changes in mouse models of E. coli infection

2.4.1. Observation of the effect of HE staining (hematoxylin-eosin staining) on the organs of mice

After collectinged the heart, lung, liver, spleen, and kidney tissues of infected mice, they were washed with Physiological saline and fixed with 4% formaldehyde fixative solution. After being soaked for 24 h, the fixed heart, lung, liver, spleen and kidney were dehydrated. Paraffin embedding, section, HE staining, microscopic image collection and pathological section analysis were completed by Chengdu Lilai Biotechnology Co., Ltd.

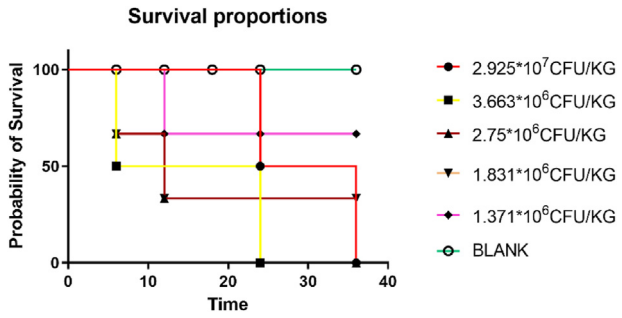

Figure 1. Survival proportions of *Escherichia coli* infection in mice.

2.4.2. Transmission electron microscope observation of the effect on mice organelles

The samples were pre-fixed with 2.5% glutaraldehyde, rinsed 3 times with 0.1M phosphoric acid rinsing solution, and fixed with 1% osmium tetroxide after 15 min each time. The samples were then dehydrated step by step with acetone with a concentration gradient of 30% → 50% → 70% → 80% → 90% → 95% → 100% (change 3 times in 100% concentration). The tissues were embedded in pure acetone and embedding solution (2:1) at room temperature for 3–4 h and then sliced by ultramicro cutting machine. The samples were stained with uranyl acetate and lead citrate for 15–20 min at room temperature, and then observed by JEM-1400PLUS transmission electron microscope.

2.5. Data analysis

We analyzed the statistical data and significant differences through Graphpad. $P < 0.05$ was considered statistically significant. $P < 0.01$ was considered to have significant statistical significance. $P < 0.001$ was considered to be of extremely significant statistical significance.

3. Results

3.1. The 50% lethal dose of E. coli infection in mice

Mice were infected with different amounts of *E. coli 25922*, and the survival proportions of mice within 7 days was counted, as shown in Figure 1. The median lethal dose (LD_{50}) was $1.371*10^6$ CFU/kg calculated by survival proportions. During the experiment, we observed that the death of the mice mainly occurred at 12h–24h after infection, and the survival of the mice had stabilized after 3 days.

3.2. Dynamic changes of inflammatory factors and iNOS in mice infected with E. coli

The concentrations of IL-1β, IL-6, TNF-α and iNOS in the serum of LD_{50} model mice before and 1, 3, 5, and 7 days after infection were detected, respectively. The results are shown in Figure 2, the concentration of inflammatory factors increased with time after infection in mice, but the increase rate gradually slowed down, peaked on day 7 (the concentrations of IL-1β, IL-6, TNF-α were 72.61 ng/mL, 113.58 ng/mL, 2539.10 ng/mL respectively). In contrast, iNOS concentrations peaked on the first day and were significantly different from the blank control group (****p-value<0.0001), and then decreased to a level that was indistinguishable from the blank control group.

3.3. Fluctuation of Escherichia coli in organs of mice after infection

We counted the bacterial colonies in heart, lung, spleen, kidney and liver homogenates showed on the 1st, 3rd and 7th days after the LD_{50} model mice were infected with *Escherichia coli*, all organs were infected to a greater degree, the decrease appeared on the third and fifth days, and the highest value of infected bacteria was reached on the seventh day (Figure 3).

3.4. Histopathological changes in mice model of E. coli infection

The HE staining results showed that compared with the control group, there were no obvious pathological changes in the heart, liver, and lungs (Figure 4A, 4B, 4D). Compared with the control group, the spleen showed slight dilation of the red pulp area, splenic sinusoids, stasis of red blood cells, and kidneys. The glomeruli in the cortical area were enlarged, and the renal cysts almost disappeared (Figure 4C, 4E).

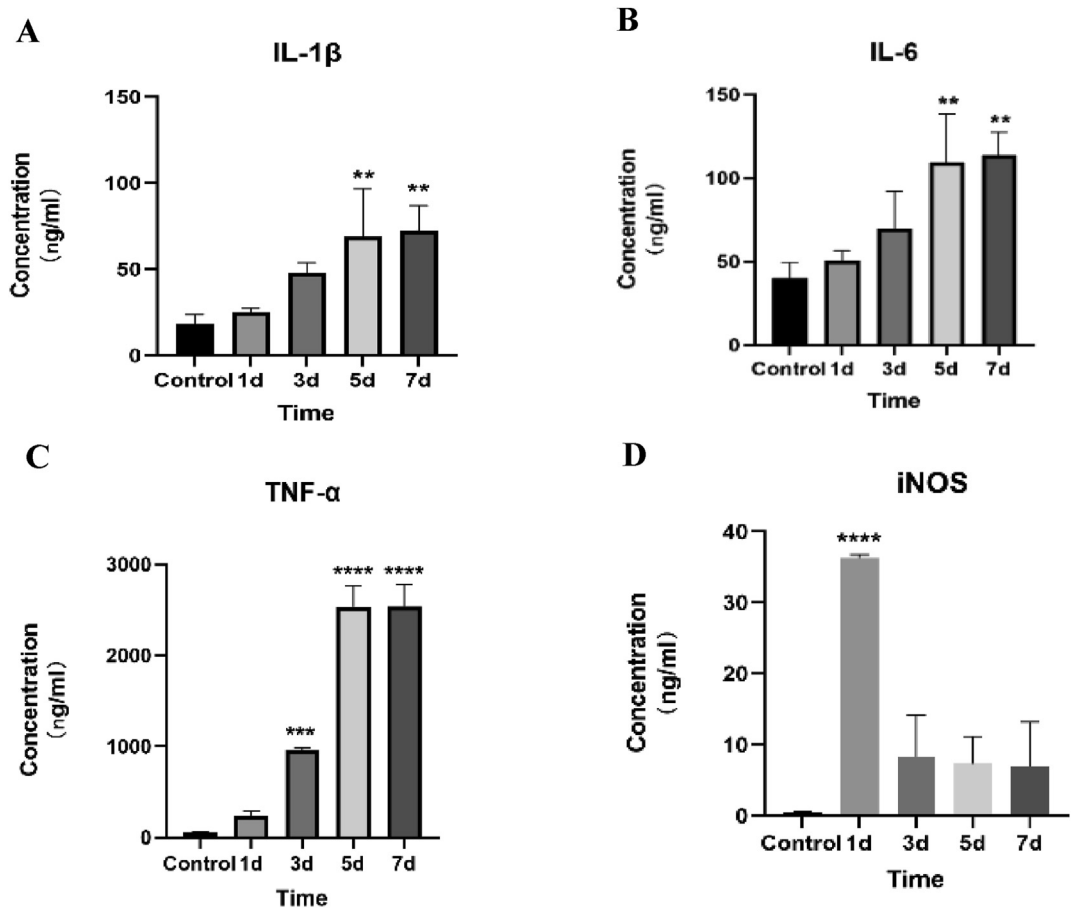

Figure 2. The concentrations of IL-1β (A), IL-6 (B), TNF-α (C) and iNOS (D) on the 1st, 3rd and 7th day after *E. coli* infection in mice.
Notes: *p-value < 0.05, **p-value < 0.01, ***p-value < 0.001, ****p-value < 0.0001 compared to control.

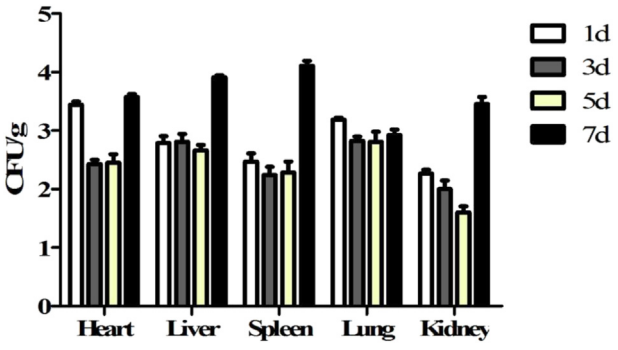

Figure 3. Bacterial load in different organs of mice for 1st, 3rd and 7th days after the LD_{50} model mice were infected with *Escherichia coli*.

Transmission Electron Microscope (TEM) results showed that compared with the control group, the experimental groups had no obvious pathological changes in the heart and liver (Figure 5A, 5B), but there were abnormal structures in the spleen, lungs and kidneys. Lymphocytes were clearly seen in the spleen. The nuclei were large and polygonal. The chromatin distribution was relatively uniform, mainly heterochromatin. The nuclear membrane was clear and intact, but the mitochondrial cytoplasm was abnormally swollen. The visual field shows the characteristics of necrotic cells, namely nuclear chromatin loss, mitochondrial swelling, autophagy and dilatation of rough endoplasmic reticulum (Figure 5C). The structure of alveolar type II epithelial cells was intact, but most of the mitochondria swelled, the crest ruptured and even disappeared, some of the rough endoplasmic reticulum dilated into sacs, and the lamellar corpuscles were fragmented or dissolved and cavitated (Figure 5D). The nuclei of renal tubular epithelial cells were oval, the structure was complete and clear, a few mitochondria were slightly swollen, and a small amount of secondary lysosomes and autophagy could be seen (Figure 5E).

4. Discussion

In recent years, drug-resistant *E. coli* has become a major and increasingly serious public health problem [11, 12, 13]. Therefore, the clinic is also facing the limitation and passive situation of the medication of *Escherichia coli*. The mouse model of *Escherichia coli* infection can be used to study the disease process and factors, so that the clinic can have a better understanding of the in vivo infection caused by *Escherichia coli* and lay a theoretical foundation for drug research and development.

In the experiment, we injected *Escherichia coli* into mice and found that the LD_{50} of *Escherichia coli* was $1.371*10^6$ CFU/kg. The tissues of mice were taken for colony count on the 1st, 3rd, 5th and 7th day after injection of LD50 of *Escherichia coli*. We found that all organs were infected to a greater degree, the decrease appeared on the third and fifth days, and the highest value of infected bacteria was reached on the seventh day. The lethal dose of *Escherichia coli* and the invasion of bacteria to the tissue of mice after injection of *Escherichia coli*, which laid the foundation for the follow-up experiment.

It is generally known that inflammatory phagocytosis of pathogenic microorganisms and non-inflammatory phagocytosis of apoptosis are the result of innate immune recognition [14]. The concentration of inflammatory factors in mice can reflect the degree of immune response of the body. Among them, IL-1β is an effective cell pro-inflammatory factor.

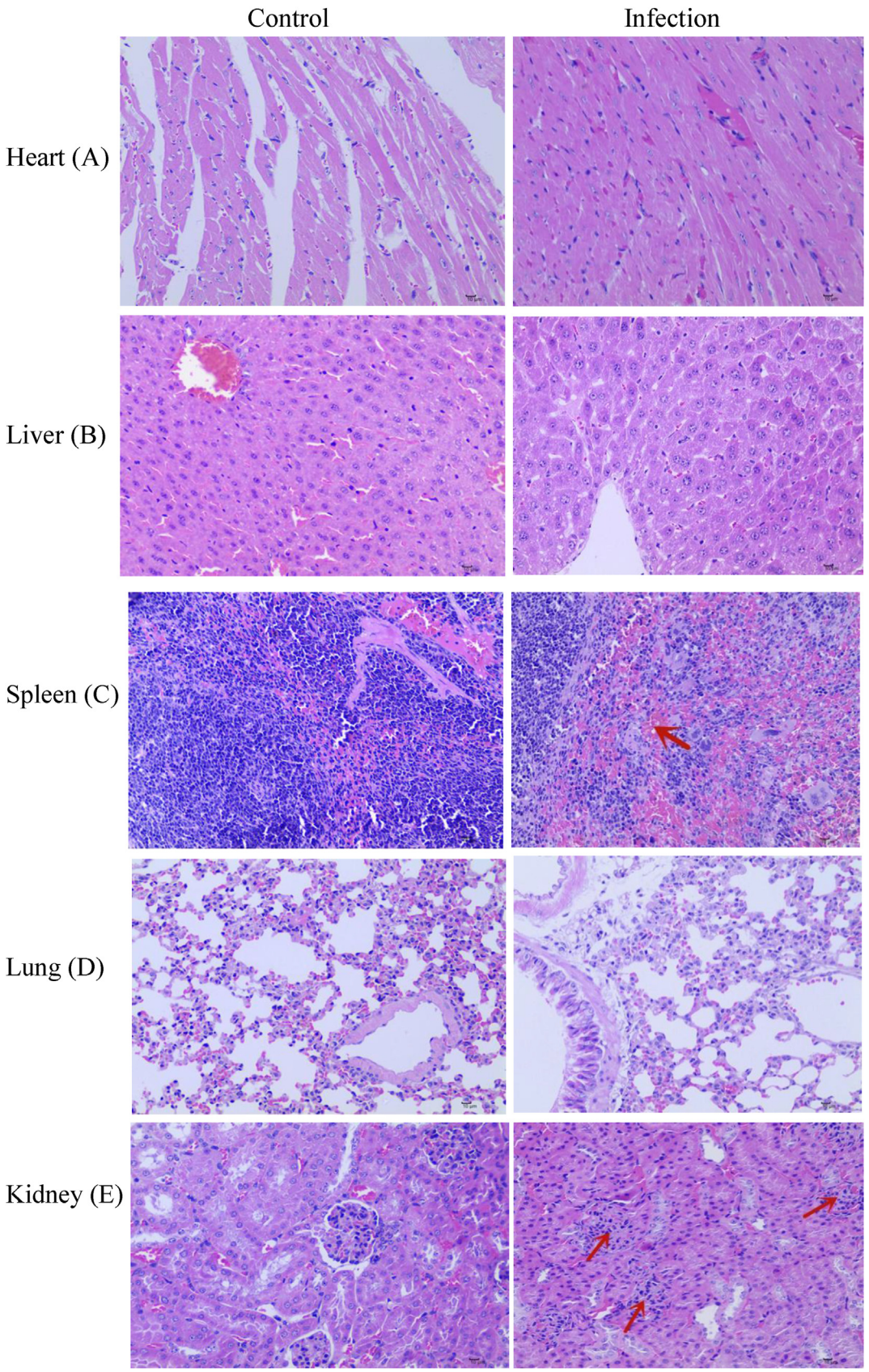

Figure 4. The comparison of HE staining in Heart (A), Liver (B), Spleen (C), Lung (D) and Kidney (E) of normal mice and *Escherichia coli* infected mice.
Notes: *E. coli* infection on internal organs revealed by HE staining. In Spleen tissue, "↑" represents Mild splenic sinus congestion. In Kidney tissue, "↑" represents Glomerular enlargement.

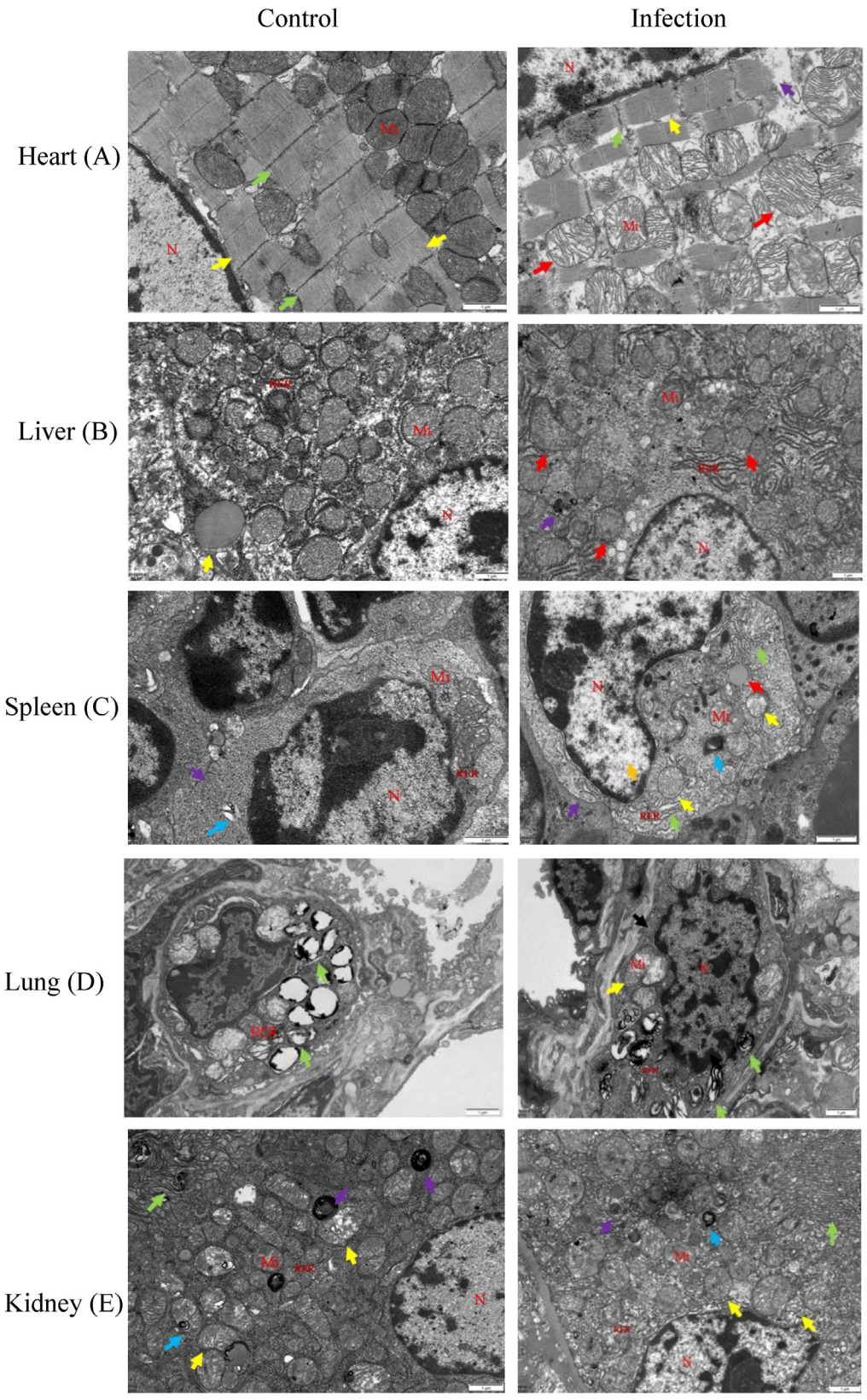

Figure 5. The comparison of TEM examination in Heart (A), Liver (B), Spleen (C), Lung (D) and Kidney (E) of normal mice and *Escherichia coli* infected mice. Notes: *E. coli* infection on internal organs revealed by TEM examination. In Heart tissue, "↑" represents Dark band., "↑" represents Z line, "↑" represents Mitochondrial swelling, "↑" represents Myofibril lysis; In Liver tissue, "↑" represents Lipid droplets, "↑" represents Mitochondrial swelling, "↑" represents Autophagy; In Spleen tissue, "↑" represents Normal lymphocytes, "↑" represents Autophagy, "↑" represents Mitochondrial swelling; In Lung tissue, "↑" represents Mitochondrial swelling, "↑" represents Lamellar body fragmentation or dissolution cavitation; In Kidney tissue, "↑" represents Mitochondrial swelling, "↑" represents Autophagy, "↑" represents Secondary lysosome, "↑" represents Brush border.

When the body is infected or injured, its defense response can effectively stimulate the body to produce an immune response [15], but it can also aggravate chronic diseases and acute tissue damage [16], Clinicians can use the value produced by IL-1β for reference to target medications, such as inhibiting the synthesis of caspase-1 to inhibit the release of IL-1β [15], so as to reduce the damage to the body. IL-6 mainly plays a role in maintaining homeostasis in vivo. When homeostasis is destroyed by infection or tissue damage, IL-6 will help the host resist this emergency stress by activating the immune response. However, when the body appears acute systemic inflammatory response syndrome and chronic immune-mediated diseases, the excessive and continuous synthesis of IL-6 will cause the body to produce a pathological response [17]. At present, some studies have suggested that IL-6 can be used as an indicator for early diagnosis of sepsis [18]. TNF-α is a pro-inflammatory cytokine. It was usually undetectable in healthy people. However, under inflammation and infection conditions, the levels of TNF-α in serum and tissue will increase and cause inflammation, which can remove irritants and accelerate tissue regeneration, but it may also cause tissue damage, and in severe cases, it may even lead to organ failure and death [10]. In addition, the concentration of iNOS reflects the oxidative stress level of the body under stimulating conditions to a certain extent [19].

Clinical bacterial infections are mainly diagnosed by blood tests and tissue biopsies, inflammatory infiltration of organs was evident after most bacterial infections [20, 21]. In this infection model, we found that different degrees of mitochondrial swelling and autophagy were observed in the spleen, kidney and lung tissues under the transmission electron microscope. Mitochondrial swelling signals cell damage and death. Combined with the pathological changes of the spleen, lung and kidney tissues of the mice in the experimental results, it is guessed whether the pathological damage of the mouse tissue after *E. coli* infection is due to the rise of inflammatory factors?

In this study, we discover *E. coli* can cause inflammation and oxidative stress in mice, causing *differen* cause different degrees of damage to the spleen, lung, and kidney tissues of the body, through this experiment, we can provided theoretical data support for inflammatory and pathological changes in vivo after *Escherichia coli* infection, and lay the foundation for more in-depth scientific research.

Declarations

Author contribution statement

Nana Long: Conceived and designed the experiments; Analyzed and interpreted the data; Wrote the paper.

Jingzhu Deng: Performed the experiments; Wrote the paper.

Min Qiu: Performed the experiments.

Yanjiao Zhang: Performed the experiments.

Yuzhen Wang: Performed the experiments.

Wei Guo: Analyzed and interpreted the data.

Min Dai: Conceived and designed the experiments.

Lin Lin: Contributed reagents, materials, analysis tools or data.

Funding statement

Professor Min Dai was supported by National Natural Science Foundation of China [31970137], Open Research Subject of Key Laboratory (Research Base) of Food Biotechnology [szjj2015-011], Sichuan Provincial Key Laboratory of Shock and Vibration of Engineering Materials and Structures, Southwest University of Science and Technology [16ZB0285], Sichuan Science and Technology Program [2020JDRC0071].

Nana Long was supported by Scientific Research Fund of Chengdu Medical College [CYZ15-02], the special project of Liyan workshop aesthetic medicine research center of chengdu medical college [21YM007].

Wei Guo was supported by the Sichuan Science and Technology Program [2020YJ0401], Project funded by China Postdoctoral Science Foundation [2021M703134].

Data availability statement

Data included in article/supp. material/referenced in article.

Declaration of interest's statement

The authors declare no conflict of interest.

Additional information

No additional information is available for this paper.

Acknowledgements

Thanks to the National Natural Science Foundation of China, Sichuan Provincial Department of Science and Technology and the Chengdu Medical College Foundation Committee for their support to the project.

References

[1] J.B. Kaper, J.P. Nataro, H.L. Mobley, Pathogenic Escherichia coli, Nat. Rev. Microbiol. 2 (2004) 123–140.

[2] J. Xia, J. Gao, W. Tang, Nosocomial infection and its molecular mechanisms of antibiotic resistance, Biosci. Trends 10 (1) (2016) 14–21. https://pubmed.ncbi.nlm.nih.gov/26877142/.

[3] J. Jang, H.G. Hur, M.J. Sadowsky, M.N. Byappanahalli, T. Yan, S. Ishii, Environmental Escherichia coli: ecology and public health implications-a review, J. Appl. Microbiol. 123 (3) (2017) 570–581.

[4] R. Wang, Y. Liu, Q. Zhang, L. Jin, Q. Wang, Y. Zhang, et al., The prevalence of colistin resistance in Escherichia coli and Klebsiella pneumoniae isolated from food animals in China: coexistence of mcr-1 and *blaNDM* with low fitness cost, Int. J. Antimicrob. Agents 51 (5) (2018) 739–744.

[5] Y. Paitan, Current trends in antimicrobial resistance of Escherichia coli, Curr. Top. Microbiol. Immunol. 416 (2018) 181–211.

[6] K.B. Tuem, A.K. Gebre, T.M. Atey, H. Bitew, E.M. Yimer, D.F. Berhe, Drug resistance patterns of Escherichia coli in Ethiopia: a meta-analysis, BioMed Res. Int. 2018 (2018), 4536905. https://www.ncbi.nlm.nih.gov/pmc/articles/pmid/29854757/.

[7] T.C. Dawson, M.A. Beck, W.A. Kuziel, F. Henderson, N. Maeda, Contrasting effects of CCR5 and CCR2 deficiency in the pulmonary inflammatory response to influenza, Virus 156 (6) (2000) 1951–1959. https://www.ncbi.nlm.nih.gov/pmc/articles/PMC1850091/.

[8] S. Herold, M. Steinmueller, W. Wulffen, L. Cakarova, R. Pinto, S. Pleschka, et al., Lung epithelial apoptosis in influenza virus pneumonia: the role of macrophage-expressed TNF-related apoptosis-inducing ligand, J. Exp. Med. 205 (13) (2008) 3065–3077. https://www.ncbi.nlm.nih.gov/pmc/articles/PMC2605231/.

[9] E. Ahmadzadeh, H. Zarkesh-Esfahani, R. Roghanian, F.N. Akbar, Comparison of Helicobacter pylori and Escherichia coli in induction of TNF-alpha mRNA from human peripheral blood mononuclear cells, Indian J. Med. Microbiol. 28 (2010) 233–237. https://linkinghub.elsevier.com/retrieve/pii/IndianJMedMicro biol_2010_28_3_233_66482.

[10] A. Kumar, K.P. Singh, P. Bali, S. Anwar, A. Kaul, O.P. Singh, et al., iNOS polymorphism modulates iNOS/NO expression via impaired antioxidant and ROS content in P. vivax and P. falciparum infection, Redox Biol. 15 (2018) 192–206. https://www.ncbi.nlm.nih.gov/pmc/articles/PMC5738204/.

[11] N. Allocati, M. Masulli, M.F. Alexeyev, C. Di Ilio, Escherichia coli in Europe: an overview, Int. J. Environ. Res. Publ. Health 10 (12) (2013) 6235–6254.

[12] The Evolving Threat of Antimicrobial Resistance: Options for Action, World Health Organization, Geneva, Switzerland, 2012. https://apps.who.int/iris/handle/10665/44812?locale-attribute=es&show=full.

[13] B.T. Huynh, M. Padget, B. Garin, P. Herindrainy, E. Kermorvant-Duchemin, L. Watier, et al., Burden of bacterial resistance among neonatal infections in low income countries: how convincing is the epidemiological evidence? BMC Infect. Dis. 15 (2015) 127. https://www.ncbi.nlm.nih.gov/pmc/articles/PMC4364576/.

[14] Miriam Beer Torchinsky, Johan Garaude, J. Magarian Blander, Infection and apoptosis as a combined inflammatory trigger, Curr. Opin. Immunol. 22 (1) (2010) 55–62. https://www.ncbi.nlm.nih.gov/pmc/articles/PMC5800876/.

[15] G. Lopez-Castejon, D. Brough, Understanding the mechanism of IL-1β secretion, Cytokine Growth Factor Rev. 22 (4) (2011) 189–195. https://www.ncbi.nlm.nih.gov/pmc/articles/PMC3714593/.

[16] C.A. Dinarello, Anti-inflammatory agents: present and future, Cell 140 (6) (2010) 935–950.

[17] T. Tanaka, M. Narazaki, T. Kishimoto, Interleukin (IL-6) immunotherapy, Cold Spring Harbor Perspect. Biol. 10 (8) (2018) a028456. https://www.ncbi.nlm.nih.gov/pmc/articles/PMC3752337/.

[18] D.J. Stearns-Kurosawa, M.F. Osuchowski, C. Valentine, S. Kurosawa, D.G. Remick, The pathogenesis of sepsis, Annu. Rev. Pathol. 6 (2011) 19–48. https://www.ncbi.nlm.nih.gov/pmc/articles/PMC3684427/.

[19] Q. Xue, Y. Yan, R. Zhang, H. Xiong, Regulation of iNOS on immune cells and its role in diseases, Int. J. Mol. Sci. 19 (12) (2018) 3805. https://www.ncbi.nlm.nih.gov/pmc/articles/PMC6320759/.

[20] Polvoy Ilona, R. Flavell Robert, Ohliger Michael, Oren Rosenberg, M. Wilson David, Nuclear imaging of bacterial infection- state of the art and future directions, J. Nucl. Med. 12 (61) (2020) 1708–1716.

[21] Zu Yan, Yan Liang, Tao Wang, Dongqing Ma, Xinghua Dong, Zhen Du, et al., A Bi2S3@mSiO2@Ag nanocomposite for enhanced CT visualization and antibacterial response in the gastrointestinal tract, J. Mater. Chem. B 4 (8) (2020) 666–676.